

# New methods for predicting and measuring dispersion in rivers

Jonathan Nelson<sup>1,\*</sup>, Richard McDonald<sup>1</sup>, Carl Legleiter<sup>1</sup>, Paul Kinzel<sup>1</sup>, Travis Terrell-Ramos<sup>1</sup>, Yutaka Higashi<sup>2</sup>, Il Won Seo<sup>3</sup>, Donghae Baek<sup>3</sup>, Du Han Lee<sup>4</sup>, and Yonguk Ryu<sup>4</sup>

<sup>1</sup>United States Geological Survey, Geomorphology and Sediment Transport Laboratory, Golden, Colorado, 80403, USA

<sup>2</sup>Kyoto University, Department of Civil Engineering, Kyoto, Japan

<sup>3</sup>Seoul National University, Department of Civil and Environmental Engineering, Seoul, South Korea

<sup>4</sup>Korean Institute for Civil Engineering and Construction Technology, Andong, South Korea

**Abstract.** To develop a better predictive tool for dispersion in rivers over a range of temporal and spatial scales, our group has developed a simple Lagrangian model that is applicable for a wide range of coordinate systems and flow modeling methodologies. The approach allows dispersion computations for a large suite of discretizations, model dimensions (1-, 2-, or 3-dimensional), spatial and temporal discretization, and turbulence closures. As the model is based on a discrete non-interacting particle approach, parallelization is straightforward, such that simulations with large numbers of particles are tractable. Results from the approach are compared to dispersion measurements made with conventional Rhodamine WT dye experiment in which typical at-a-point sensors are employed to determine concentration. The model performs well, but spatial resolution for experiments over large and or complex river flows was inadequate for model testing. To address this issue, we explored the idea of measuring spatial concentrations in river flows using hyperspectral remote sensing. Experiments both for idealized channels and real rivers show that this technique is viable and can provide high levels of spatial detail in concentration measurements with quantitatively accurate concentrations.

## 1. Introduction

Dispersion in rivers is a critically important part of many important physical and biological problems, including predicting temperature patterns, tracking pollutants, and estimating drift of nutrients and larval fish in rivers. In the past, this problem has been treated using relatively simple flow models coupled to concentration computations that employ empirical dispersion coefficients to represent the effect of higher-order fluid mechanical effects, such as dispersion by secondary flows, turbulence, and storage zones. Because of the need for a better physical representation of this problem, our group has developed a general purpose Lagrangian dispersion model that can be used with a wide spectrum of flow models that capture flow physics at differing levels of accuracy. The model is based on a parallelized

---

\* Corresponding author: [jmn@usgs.gov](mailto:jmn@usgs.gov)

code that calculates the advection of particles using the flow solution plus a simple random walk algorithm based on the local turbulent diffusivity from the flow model. This allows examination of the specific physical effects represented by different models. For example, if we use a completely two-dimensional flow solution for one dispersion calculation, and a three-dimensional calculation in another, the effects of vertical shears and secondary flows can be examined. Similarly, using a three-dimensional calculation with different turbulence closures (e.g., isotropic vs anisotropic), the effects on dispersion predictions can be seen by comparison of the two results and the better approach can be judged by comparison to field data. Because the Lagrangian particle-tracking approach is perfectly parallel, as there is no interaction between advected particles or between the particles and the flow, the approach is computationally efficient and can incorporate millions of particles, as required for results with high spatial resolution.

To test our approach, we collected data on dispersion from several rivers with conventional techniques using Rhodamine WT dye injections and sondes for measuring dye concentration. Comparison of the sonde measurements with results from the Lagrangian modeling approach shows that the model does a good job of predicting concentrations provided that the spatial resolution of the model is sufficient to capture river bathymetry and bank irregularities, which both play an important role in the bulk dispersion. However, the comparison is not a complete test, as one of the shortcomings of using concentration measurements at single points is that the details of spatial concentration patterns are not well resolved, so comparisons can only be done at the few spatial points where sondes are located. To deal with this issue, we have been exploring the use of hyperspectral and conventional imagery for quantitative predictions of spatially distributed dye concentration at two sites, first using a drone on a relatively simple experimental channel at the Korea Institute for Civil Engineering and Construction Technology (KICT) Andong River Experiment Center (REC) and subsequently using manned aircraft on the Kootenai River, a large meandering river in northern Idaho. In both cases, the optical techniques were successful. For the hyperspectral approach, simple band ratios using the Rhodamine WT emission wavelength gave extremely good correlations, with  $r$ -squared values typically greater than 0.9. In addition, the low concentration or detectability level of the hyperspectral was actually better than that of the sondes, with minimum level of detectability well below 1 part per billion. Comparing the spatially distributed concentration results with model predictions still shows good agreement and (using different flow models) helps to explain the role of various physical approaches in producing dispersion. Together, the new measurement technology strongly complements the modeling approach, in that both allow unprecedented examination of spatial distributions of concentration and a more complete view of the important physical processes acting to produce dispersion in rivers.

In this paper, we present a brief description of the Lagrangian computational model, some comparisons with conventional dye measurements, and then go on to briefly discuss the remote sensing method for spatially-detailed concentration measurements.

## 2. Model Development

Generally, models for dispersion in rivers are constructed as a subcomponent of a riverine flow model, because high-resolution advective velocities are required. Because of this coupling of approaches, the dispersion method is typically constructed with a single specific grid or mesh structure to match the flow model. For the case here, our intent was to build a single Lagrangian approach that would work with a wide variety of flow models, and in particular we considered the suite of models available in the public-domain iRIC flow modeling interface ([www.i-ric.org](http://www.i-ric.org), [1]). The models within the iRIC system span the range from 1-dimensional to 3-dimensional, include both quasi-steady and fully unsteady models,

and also cover a wide range of turbulence treatments including several closure techniques as well as large-eddy simulation. The aim of computing Lagrangian dispersion over a wide range of flow models was to provide direct assessments of differing physical treatments and assumptions, as well as allowing more sophisticated models to aid in understanding the dispersion used by simpler models that average over spatial dimensions or various parts of the turbulence spectrum. The fundamental component of this approach is a methodology that both keeps track of the location of advected particles and also determines appropriate velocities and diffusivities from the model-predicted flow field. Notably, this information must be found for a wide range of spatially distributed points, in some cases from orthogonal or general grids and in others from a variety of finite element or volume meshes depending on the flow computation methodology. We tried a variety of search methods for this part of the problem, and found that the most efficient approach was the cell selection and interpolation method found in the Virtual Toolkit (VTK), which employs an octree subdivision technique described in [2].

Provided that the step lengths of each particle are small relative to the resolution of the grid, the dispersion scales and the flow depth, the movement of the particles can be readily computed as the sum of advection and dispersion. For example, given a particle at a vector position  $\mathbf{r}$ , the position of the particle at a small time step,  $\Delta t$ , in the future can be written as follows:

$$\mathbf{r}(t+\Delta t) = \mathbf{r}(t) + \mathbf{u}(\Delta t) + \mathbf{L}\sqrt{2K\Delta t} \tag{1}$$

where  $\mathbf{u}$  is the vector velocity,  $K$  is the (presumed isotropic) diffusivity taken from the flow model, and  $\mathbf{L}$  is a vector, each component of which is randomly chosen from a Gaussian distribution with a mean of zero and a standard deviation of one. Note that if the time step is not small relative to the time required for traversal of model cells, better interpolation of the velocity may be required and terms associated with spatial gradients of dispersion and depth may appear in Equation (1). In our calculations, the time step is much smaller than the cell traversal time and this equation is sufficient (see the discussion by Callies [3]). This equation represents completely passive movement of a particle through a turbulent flow; if the particle has some active behaviour, such as swimming or maintaining position at a given depth, an active component of velocity or position can be added to this equation. For flow models that give anisotropic diffusivities (e.g., NaysCube in iRIC), the last term in Equation (1) can be replaced with three terms, each with a separate diffusivity corresponding to the coordinate directions.

Although Equation (1) is written for a three-dimensional flow, it can be readily reduced to a two or one-dimensional situation, in which case only the appropriate velocity and random walk components are incorporated. For example, in a two-dimensional vertically averaged flow field,  $\mathbf{u}$  has components of the vertical averaged flow only in two directions and  $\mathbf{L}$  has only two random walk components; in a one-dimensional case,  $\mathbf{u}$  and  $\mathbf{L}$  have only one component corresponding to cross-sectionally averaged velocity and one-dimensional dispersion. The value of  $K$  also changes across this range of model resolution, typically increasing as the dimensionality decreases and progressively more detailed physical effects are pushed into the dispersion term because they are unresolved by the modeling method. Thus, the method we describe is sufficiently general to work with a variety of modeling approaches.

For practical computations, the user selects the initial position of dispersed particles and steps forward in time to predict their movement. Initial particle positions can include a continuous source or a single emplacement of tracers. For the cases shown here, the initial condition was a single pulse of particles at one location. Because particles do not interact or have any feedback on the flow field, the computational task is simple to parallelize. For small

simulations (such as for laboratory flumes or small streams) calculations typical require only 10,000 particles or so, but for long reaches of real rivers with complex banks, the requirement for spatial resolution of the concentration field can easily reach many millions of particles, in which case parallel computations are necessary for reasonable run times. Over the course of the computations, all particle tracks are recorded along with particle counts per computational cell over the run period, as will be discussed in more detail below.

### 3. Field Measurements

To test the methodology described above, several experiments were carried out using passive dye (Rhodamine WT, [4]) tracers in both real rivers and man-made experimental channels. In this paper, two of these studies are briefly described, one for the Kootenai River in northern Idaho and the other for an experimental meandering channel at the River Experiment Center (REC) in Andong, South Korea. In both cases, dye concentration measurements were made using calibrated sondes at several points in the experimental domain. Kootenai River concentration observations are in [5], REC observations are available from KICT.

The Kootenai River site was chosen because we hoped to use the passive dye measurements to verify the modeling approach and then use that approach with simple active behaviour assumptions to consider larval sturgeon drift. This work is part of an ongoing collaborative effort among various agencies and the Kootenai Tribe of Idaho to restore native fisheries in the Kootenai through a large-scale restoration effort.

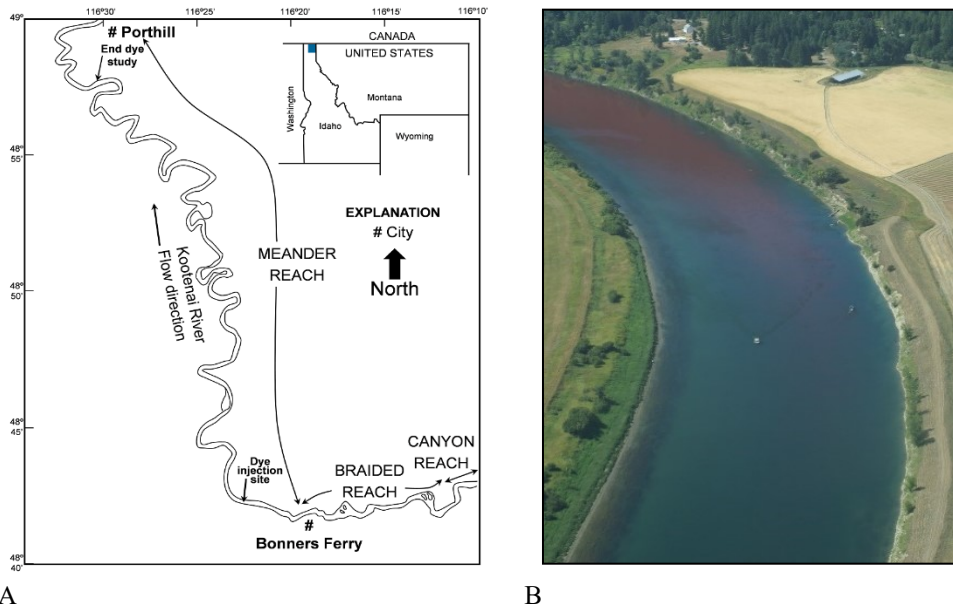


**Fig. 1.** A. Schematic diagram of the Kootenai River dye study showing injection point and the entire study reach. B. Aerial photograph of the dye cloud in the Kootenai River.

Figure 1 shows the experimental site and a photo of the dye moving down the Kootenai River. Over the two-day period of the study, sondes collected concentration at discrete points; we also collected some cross-sectional concentration data using a sonde with a slow-moving boat traversing back and forth across the river. Sonde locations were chosen with results of previous dye studies at this location in mind in order to locate the sondes within the dye

cloud. This produces some bias but also ensures that the most information about the dye cloud is obtained from a the 12 sondes.

An aerial view of the second site is shown in Figure 2. This simple meandering channel is a man-made channel located at the REC developed by the Korean Institute for Civil Engineering and Building Technology (KICT). The entire channel has similar bends of three different amplitudes but only one of the three is shown in Figure 2; this is the bend on which our concentration measurements were focused. As in the Kootenai, measurements were made using an array of sondes and a single pulse of dye added upstream of the bend shown.

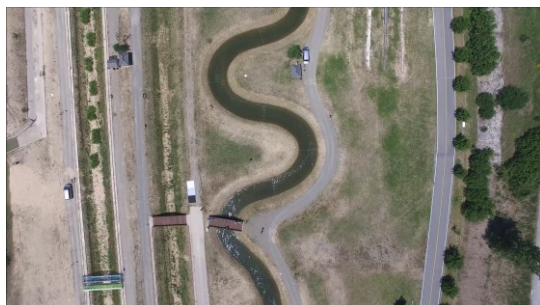


**Fig. 2.** Study site on the manmade channel at the KICT River Experiment Center in South Korea. Note vehicles and pedestrians for scale.

## 4. Results and Discussion

Because both measurement sites were on channels with strong curvature, suggesting that secondary flows and the associated shear dispersion would likely be important, our initial computations were carried out with a quasi-steady, quasi-three-dimensional model FaSTMECH [1, 6]. This approach provides vertical structure, including the effects of secondary flows, but neglects unsteadiness except that associated with discharge changes (the hydrograph). The turbulence closure is simple and standard, with the horizontal diffusivity ( $K_H$ ) given by the following:

$$K_H = \frac{ku_*h}{6.9} + LEV \quad (2)$$

where  $k$  is von Karmann’s coefficient ( $=0.4$ ),  $u_*$  is the local shear velocity,  $h$  is the local depth, and LEV is a lateral eddy viscosity correction term representing the effect of untreated horizontal flow unsteadiness. This value was set to  $0.225\text{m}^2/\text{s}$  for the Kootenai River runs and  $0.01\text{m}^2/\text{s}$  for the calculations for the meandering channel at the REC. Using  $z$  as the vertical coordinate, the vertical diffusivity ( $K_z$ ) in FaSTMECH is given by the Rattray-Mitsuda [7] best-fit profile:

$$K_z = ku_*z\left(1 - \frac{z}{h}\right) \quad z \leq 0.2h \quad (3)$$

$$K_z = \frac{ku_*h}{6.25} \quad z > 0.2h \quad (4)$$

Because the local vertical diffusivity is constant over most of the flow depth, we use only the vertically averaged value of  $K_z$  over the entire flow depth, which has a negligible effect on the particle tracking solution, especially because the vertical gradients in concentration tend to become negligibly small except in the near field region of the particle or dye release. Figure 3 shows a single frame of a typical particle tracking result over a short reach of river. In these calculations, the total volume of dye is divided by the total number of tracked particles such that each particle represents a specific amount of dye. This normalization must be done to

make quantitative comparisons of measured and predicted concentration. Model results are available in detail in [8].

Figure 4 shows a comparison between measured and predicted dye concentrations at three locations along the study reach on the Kootenai River. The match between the measured and predicted values is good, but comparisons of measured and modelled values at only a few locations in the main part of the channel can be misleading. For example, when comparing at a single point, it is difficult to distinguish errors associated with under or overestimation of dispersion with differences in the location of the maximum concentration in the dye cloud in the model relative to the real situation. In Figure 4 this is addressed partially by showing that cross-sectional mean and standard deviation in the dye cloud, but this method is still insufficient, as no more information about the actual spatial distribution of the measured dye is added. Knowledge of the spatial location of the edge of the dye cloud is important for evaluating potential contamination at water intakes or other local effects.



**Fig. 3.** Single frame of particle tracking animation, where white dots are particles and orange areas represent the total particle counts in cells over the entire computation, as denoted by the color bar.

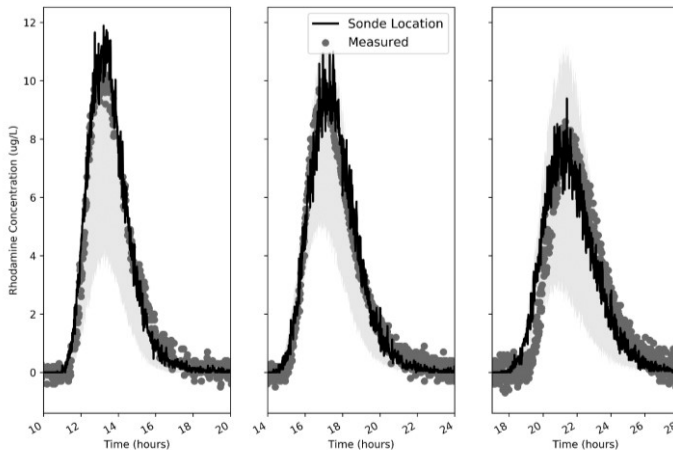


**Fig. 4.** Comparisons of measured (black lines) and modelled (grey points) at three locations in the Kootenai River approximately 16.4, 20.7, and 24.5 river km downstream from the dye injection point. The light gray shading indicated the modelled cross-sectional mean concentrations plus and minus the modelled cross-section standard deviations at the river section where the sonde was located.

During the dye study work at the REC in South Korea, photographic images and videos of the dye cloud were taken from a drone. Thus, in addition to comparisons of measured and computed concentration as specific sonde locations (which were also made and look much

like those in Fig. 4), it was possible to qualitatively compare imagery with the predicted spatial pattern of concentration, shown in Figure 5.

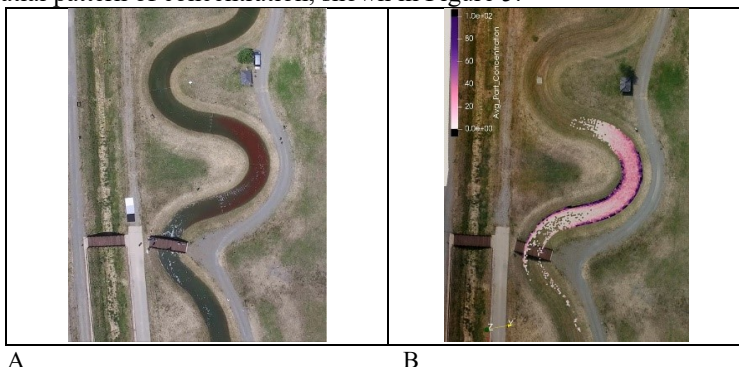


**Fig. 5.** Photo (A) and particle tracking simulation (B) of dye in the REC meandering channel.

The comparison shown suggests that a better overall test of any dispersion modeling method (including the one described here) should include some spatial comparison to better ascertain errors that an at-a-point analysis cannot provide. While visual wavelength photos videos alone may help in this regard, a more precise method that can provide quantitative accuracy is more desirable.

With this in mind and noting the optical properties of Rhodamine WT dye, we investigated using a hyperspectral scanner to try to measure detailed spatial dye concentrations. We did this first at the REC site using a drone-mounted hyperspectral scanner. Calibration was carried out using known volumes of Rhodamine in known volumes of water to perform a typical static calibration, as shown in Figure 6A.

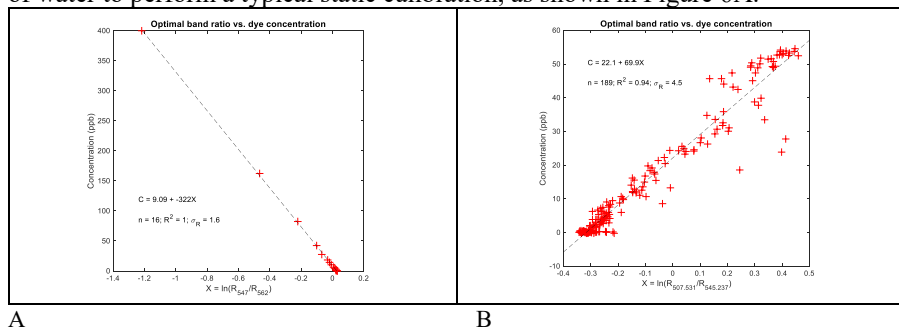


**Fig. 6.** Static (A) and dynamic (B) calibration of optimum hyperspectral band ratios (see, e.g., Legleiter et al. [8]) and Rhodamine WT dye concentration.

We also hovered the drone over specific sonde locations in the flow and carried out calibrations using the sonde-measured (dynamic) concentrations along with the contemporaneous hyperspectral data; an example is shown in Figure 6B. Figure 6A shows that the static dye concentrations are extremely well predicted by simple hyperspectral band ratio calculations [9], with an  $R^2$  value of 1.00. Notably, the lowest three concentration values measured correspond to values below the detection level of the sondes (1 ppb, typically). When the additional uncertainties of navigational positioning, orthorectification, and temporal variability are added, the calibration is not quite so perfect but still very good, with an  $R^2$  value of 0.94. These exceptional fits are a result of the very narrow emission spectrum of Rhodamine WT, which is centered on 570nm. Using the calibrations, spatial concentrations of dye were developed for the REC experiment. Figure 7 shows a comparison for a low sinuosity reach of the REC channel.

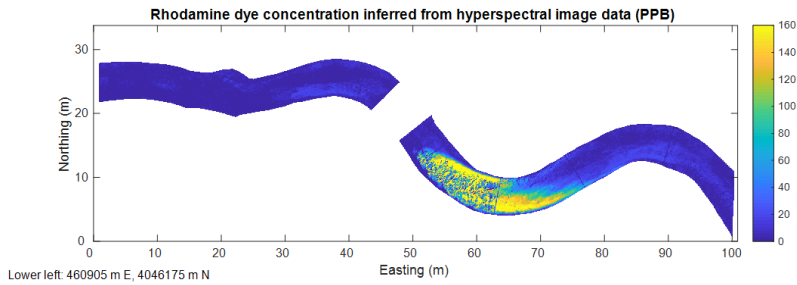


**Fig. 7.** Dye cloud inferred from hyperspectral scans made from a drone.

Although this first-level analysis of the hyperspectral data shows impacts of sun glint and probable errors associated with drone positioning and image rectification, it represents an exciting step in obtaining quantitative information on dispersion using drones with lightweight hyperspectral scanners.

## 5. Conclusions

Accurate predictions of dispersion are critically important for a wide range of practical problems. Determining the required level of computational treatment for a given problem is improved by the ability to use models of varying complexity within a single framework. The Lagrangian method we describe here provides that flexibility. During the preparation of this paper, we carried out airborne hyperspectral scanning of a full-scale dye study in a reach of the Kootenai River. Early results show promise for both the direct measurement of dispersion and the provision of detailed information for testing modeling approaches for real rivers.

The authors acknowledge support and field assistance from the Kootenai Tribe of Idaho and the South Korean government through Seoul National University and KICT. Any use of trade, firm or product name is for descriptive purposes only and does not imply endorsement by the United States government.

## References

1. J.M. Nelson, Y. Shimizu, T. Abe, K. Asahi, M. Gamou, T. Inoue, T. Iwasaki, T. Kakinuma, S. Kawamura, I. Kimura, T. Kyuka, R.R. McDonald, M. Nabi, M. Nakatsugawa, F. Simoes, H. Takebayashi, Y. Watanabe, *Advances in Water Resources*, **93**, p. 62-74. (2016)
2. W. Schroeder, K. Martin, B. Lorensen, *The Visualization Toolkit (VTK, 4th Edition)*, Kitware, ISBN-978-1-930934-19-1. (2006)
3. U. Callies, A. Pluss, J. Kappenberg, H. Kapitza, *Ocean Dynamics*, **61**, 2121. (2011)
4. Runkel, R. L., 2015, *Water Resources Research*, **51**, p. 6125–6142, DOI:10.1002/2015WR017201
5. McDonald, R.R., Nelson, J.M., Logan, B., Runkel, R.L., Kinzel, P.J., and Walton-Day, K., Rhodamine concentration data, Kootenai River, near Bonners Ferry, Idaho, 2008. U.S. Geological Survey data release, <https://doi.org/10.5066/F7S75FMH> (2018).
6. J.M. Nelson, R.R. McDonald R.R., *Mechanics and modeling of flow and bed evolution in lateral separation eddies*, Glen Canyon Environmental Studies Report, Glen Canyon Monitoring and Research Center, 69 pp. (1997)
7. M. Rattray, E. Mitsuda, *Estuarine and Coastal Marine Science*, **2**, 375-394. (1974)
8. McDonald, R.R. and Nelson, J. M., *Model Archive: Simulation of Rhodamine Dye Concentration and Larval Drift, Kootenai River, Idaho*: U.S. Geological Survey data release, <https://doi.org/10.5066/F7NV9HKC> (2018)
9. C.J. Legleiter, D.A. Roberts, R.L. Lawrence, *Earth Surface Processes and Landforms*, **34**(8), 1039-1059. (2009)